ER-5579

BRAYTON CYCLE CAVITY RECEIVER DEVELOPMENT

QUARTERLY REPORT

JULY 1963 – SEPTEMBER 1963

TAPCO
A DIVISION OF
Thompson Ramo Wooldridge Inc.
CLEVELAND, OHIO

570774

44Bs

ER-5579

BRAYTON CYCLE CAVITY RECEIVER DEVELOPMENT

QUARTERLY REPORT

Technical Management
NASA-Lewis Research Center
Solar and Chemical Power Branch
Attn.: J. A. Milko (86-1)

JULY 1963 – SEPTEMBER 1963

TAPCO
A DIVISION OF
Thompson Ramo Wooldridge Inc.
CLEVELAND, OHIO

NOTICE

This report was prepared as an account of Government-sponsored work. Neither the United States, nor the National Aeronautics and Space Administration (NASA), nor any person acting on behalf of NASA:

a. Makes any warranty or representation expressed or implied with respect to the accuracy, completeness, or usefulness of the information contained in this report, or that the use of any information, apparatus, method, or process disclosed in this report may not infringe privately-owned rights; or

b. Assumes any liabilities with respect to the use of, or for damages resulting from the use of any information, apparatus, method, or process disclosed in this report.

As used above, "person acting on behalf of NASA" includes any employee or contractor of NASA, or employee of such contractor, to the extent that such employees or contractor of NASA, or employee of such contractor prepares, disseminates, or provides access to, any information pursuant to his employment or contract with NASA, or his employment with such contractor.

Requests for copies of this report should be referred to:

National Aeronautics and Space Administration
Office of Scientific and Technical Information
Washington 25, D.C.

Attention: AFSS-A

TABLE OF CONTENTS

LIST OF ILLUSTRATIONS

1.0 PROJECT OBJECTIVES

The Brayton cycle cavity receiver development program as presently planned consists of three phases. Phase I is being perfomed currently and features both a design study of the full-scale flightweight unit and a material compatability investigation with lithium fluoride as the corrosive salt. Phase II is contemplated to consist of construction and ground test of the flightweight unit. Phase III is planned as the endurance test of the flightweight unit. The ultimate objective of the program is to demonstrate a one year endurance capability of the flightweight unit in a ground test.

2.0 PROJECT OBJECTIVES FOR THE REPORTING PERIOD OF JULY 1, 1963 THROUGH OCTOBER 1, 1963

Preliminary design analysis of the flightweight cavity receiver shall be performed and completed within two months after contract initiation.

A technical presentation setting forth the results of the preliminary design analysis shall be made to interested NASA personnel after completion of the analysis.

Small-scale experiments shall be initiated to determine:

a) the thermal conductivity of lithium fluoride in the liquid and solid states near the melting temperature,

b) possible heat input and heat release rates for various storage bath geometries, and

c) the void and freezing characteristics of lithium fluoride in the various geometries.

A study of various cavity surface temperature control and aperture closure methods shall be started on the preferred design, resulting from the preliminary design analysis.

A survey shall be conducted to determine the properties of lithium fluoride which influence the cavity receiver design, the values of these properties that are available, the discrepancies or voids that exist, and the purity, handling and safety requirements of lithium fluoride.

A reliability program shall be implemented, consistent with the contract requirements.

In the materials compatability investigation, the test materials shall be purchased, test capsules fabricated and prepared for lithium fluoride loading, test containers constructed, and the furnace prepared for operation. The first 2500-hour furnace test is scheduled to begin early in the following quarter.

3.0 PROJECT PROGRESS DURING THE REPORTING PERIOD

3.1 Preliminary Design Analysis

The major differences between the Sunflower boiler/heat storage unit and the Brayton cycle cavity receiver unit are those of the heat storage medium and the cycle working fluid. Sunflower employs lithium hydride for heat storage and mercury as the working fluid, whereas the Brayton cavity receiver is intended to feature lithium fluoride as the heat storage medium and argon as the inert gas working fluid. The melting temperature increase from 1265°F, for lithium hydride, to 1560°F, for lithium fluoride, permits the turbine to operate with an inlet temperature approaching 1500°F. Such operation is beneficial to the cycle performance.

The use of a gas as the working fluid operating within low allowable pressure drop limits means inherently low heat transfer coefficients. These coefficients are orders of magnitude less than the coefficients obtained with boiling mercury in the Sunflower design. As a result, it is no longer obvious whether the thermal resistance of the gas side or the fluoride side is higher, and therefore, controlling. This uncertainty is increased by the lack of thermal conductivity data for lithium fluoride. In view of the possibility that the gas side may be controlling and to optimize the tubing in the heater design, a parametric analysis was conducted for the design study.

The inlet and exit conditions of prime interest in the design study were specified by NASA and are listed in the following table. The weight flow rates for 30-ft diameter and 20-ft diameter collectors are also shown. The contract specifies, in addition, that a range of gas side temperatures and gas side pressure drops be considered.

SPECIFIED CONDITIONS FOR ARGON GAS

Temperature at Receiver Inlet	1446°R
Temperature at Receiver Exit	1950°R
Pressure at Receiver Inlet	13.72 psia
Pressure at Receiver Exit	13.17 psia
Flow Rate for 30-ft Diameter Collector	36.7 lb/min
Flow Rate for 20-ft Diameter Collector	14.7 lb/min

The preliminary design analysis considered three main areas:

a) heater design
b) storage bath design, and
c) cavity design

3.1.1 Heater Design

The gas side heat transfer analysis was concerned primarily with circular tubes for laminar and turbulent flow. Because of difficulties encountered in solving the geometrical prob-

lems associated with placing the required tube surface area in suitable cavity shapes, rectangular tubes were also examined for turbulent flow. The results for turbulent flow in rectangular tubes were similar to the circular tube results, with this exception: the required number of rectangular tubes was reduced, since the surface area per tube was increased.

In the analysis performed, three governing equations were obtained for each type of flow. The equations have four unknowns and thus, a unique solution is not possible. The equations, derived in Appendix II, are presented below.

Laminar Flow

$$\frac{23.544}{Re} \cdot \frac{L}{D} = \frac{\Delta t_g}{\Delta t_m}$$

$$Re \cdot \frac{L}{D} \cdot \frac{1}{D^2} = K_L$$

$$Re\,N\,D = \frac{4w}{\pi \bar{\mu}}$$

Turbulent Flow

$$\frac{0.1536\, Re^{-1/4}}{1-0.534\, Re^{-1/8}} = \frac{\Delta t_g}{\Delta t_m}$$

$$Re^{1.75}\, \frac{L}{D} \cdot \frac{1}{D^2} = K_T$$

$$Re\,N\,D = \frac{4\,w}{\pi \bar{\mu}}$$

Where Re = Reynolds Number $= \frac{GD}{\bar{\mu}}$

D = tube inside diameter, ft

L = tube length, ft

N = number of tubes

G = mass velocity, lb/sec-sq. ft

$\bar{\mu}$ = average absolute viscosity, lb/sec-ft

$\Delta t_g = t_{g,2} - t_{g,1}$ = gas side temperature difference

Δt_m = log mean temperature difference between tube wall and gas stream

K_L = laminar factor $K = \frac{2g_c}{64} \cdot \frac{\Delta P \bar{\rho}}{\bar{\mu}^2}$

ΔP = allowable pressure drop lb/sq. ft

$\bar{\rho}$ = average density, lb/cu. ft

g_c = gravitational conversion constant, $lb_f\text{-ft}/lb_m\text{-sec}^2$

K_T = turbulent factor $K = \frac{2g_c}{0.316} \cdot \frac{\Delta P \bar{\rho}}{\bar{\mu}^2}$

w = weight flow, lb/sec

With fixed quantities for the terms on the right side of the equations, the unknowns are Re, L, D, and N. Then for any given Re number, a unique solution can be obtained for N, D, and L. The tube surface area required is π NDL. Thus, the product NDL is proportional to the tube surface area and is significant. As the product NDL is reduced, a corresponding reduction in the tube surface area is obtained. Further, minimum surface area gives minimum tube volume and consequently, minimum tube weight for any given level of the factor K. Hence, a design featuring the minimum practical NDL is considered optimum.

The variation of the minimum NDL product at any given K level with the factor K_L is shown in Figure 1. The range of the factor K_L corresponds to the range of gas pressure drops and gas side temperature differences given in Figure 2. That shown in Figure 2 covers the total possible range of gas side variables for this application. Figure 1 corresponds to a constant value of the ratio $\Delta t_g/\Delta t_m$, also.

The variation of the minimum NDL product with the factor K_T is shown in Figure 3 for several levels of the $\Delta t_g/\Delta t_m$ ratio. The range of K_T in Figure 3 corresponds to the range of gas side variables illustrated in Figure 4. The range of variables in Figure 4 is the same as the range in Figure 2.

A relative comparison of laminar and turbulent flow at the same temperature ratio level can be made for any gas side temperature difference and pressure drop within the range of Figures 2 and 4. An example of interest is a gas temperature difference of 500°F and a 2 percent pressure drop. From Figure 2, $K_L = 9.5 \times 10^8$. From Figure 4, $K_T = 1.95 \times 10^{11}$. From Figure 1, NDL = 24.0 ft^2, and from Figure 3, NDL = 32 ft^2 for an equivalent temperature ratio. Thus, laminar flow indicates a potential advantage over turbulent flow of about one-third in surface area and weight. This simple comparison does not present the entire picture, however. For example, the number of tubes required in laminar flow is many times the number required in turbulent flow. Similar difficulty in packaging the number of circular tubes for turbulent flow in a suitable storage bath container led to a temporary consideration of rectangular tubes.

In the apportionment of the allowable pressure drop between headers and heater tubes, approximately one-half was assigned to the headers. If conventional headers are employed, the results presented in Reference 1 indicate that the lowest entrance total pressure loss that

VARIATION OF THE MINIMUM NDL VALUE WITH THE FACTOR K FOR LAMINAR FLOW IN CIRCULAR TUBES

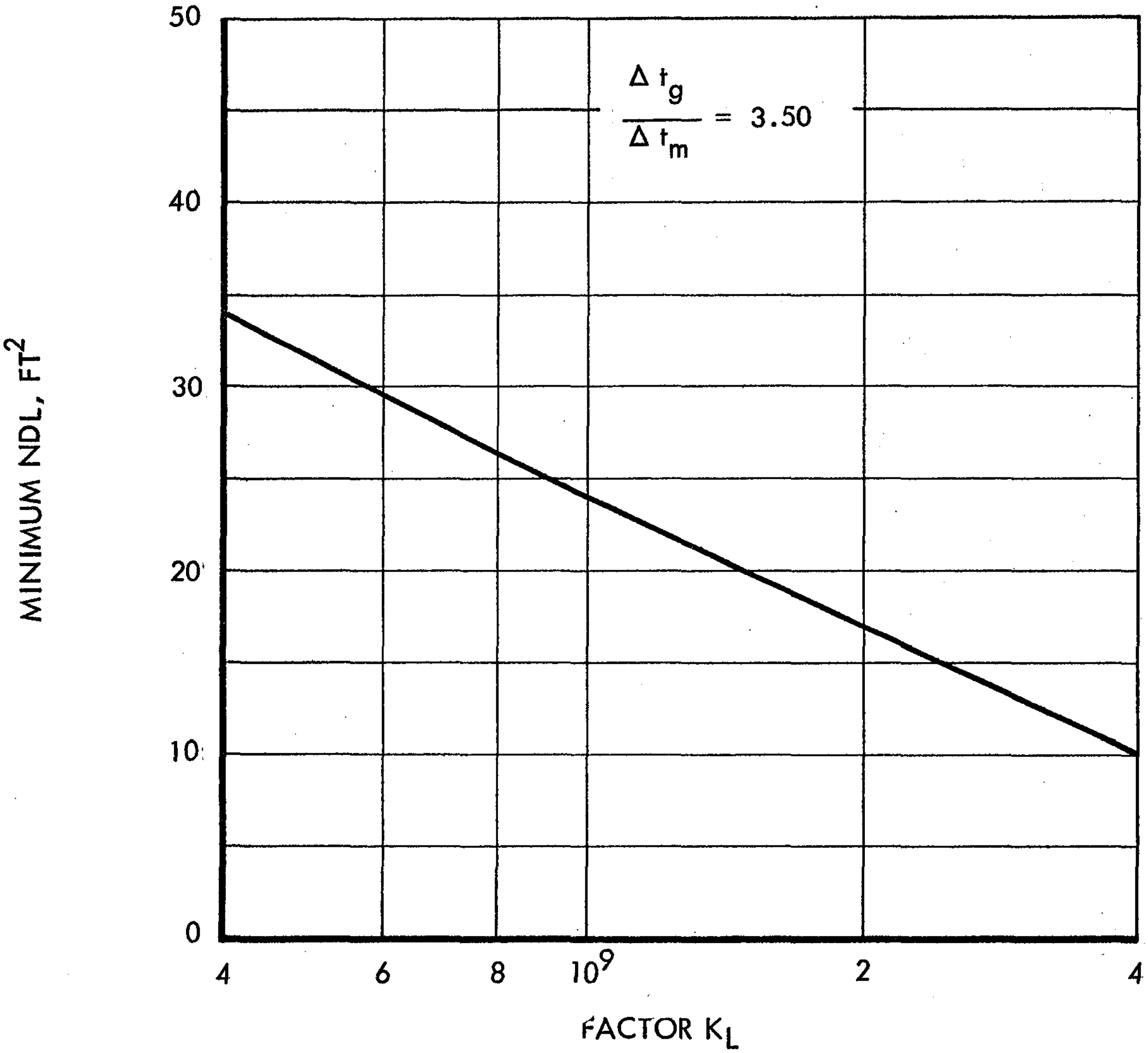

FIGURE 1

VARIATION OF THE FACTOR K FOR LAMINAR FLOW IN CIRCULAR TUBES WITH GAS SIDE TEMPERATURE DIFFERENCE AND PRESSURE DROP RATIO

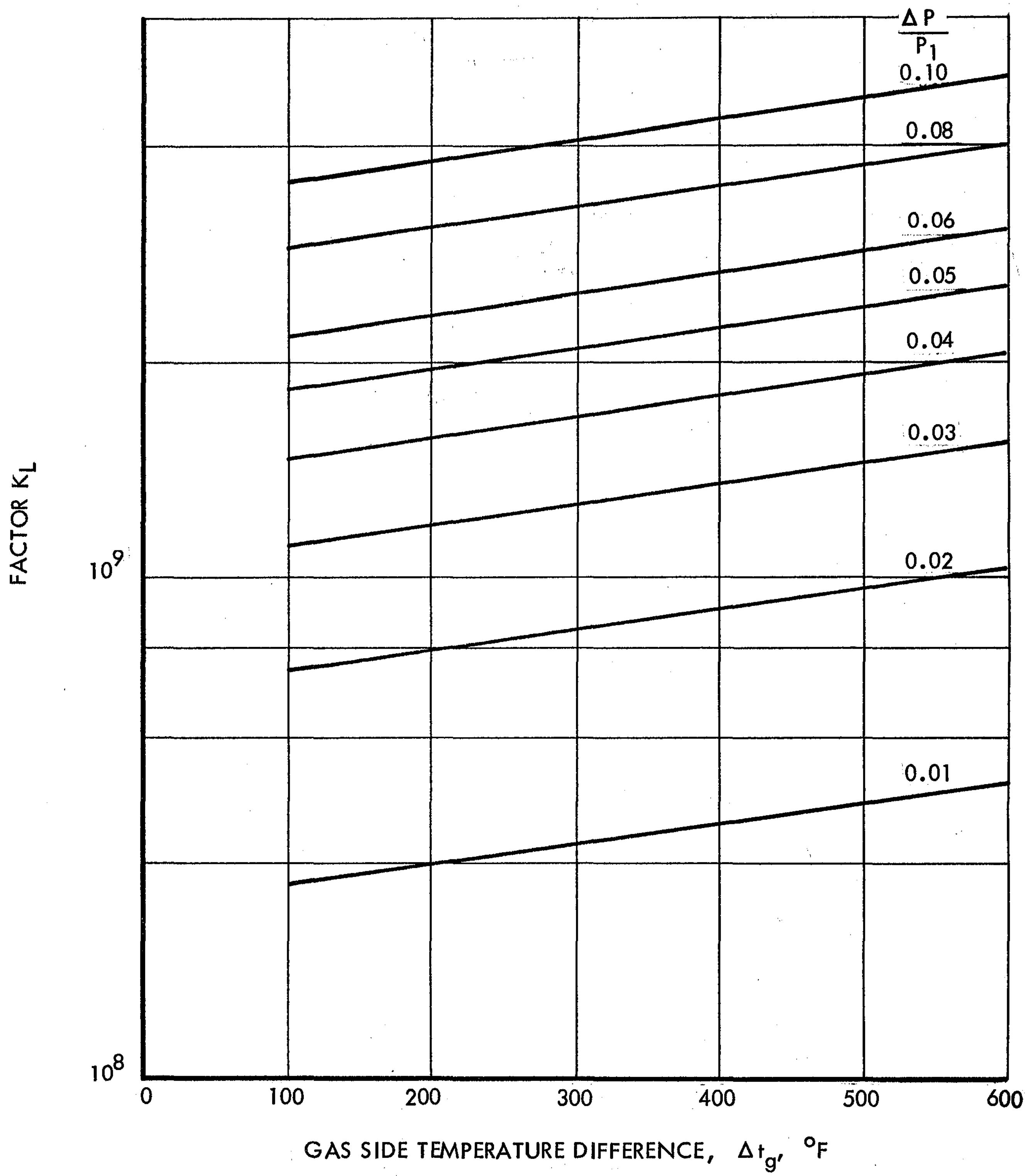

FIGURE 2

VARIATION OF THE MINIMUM NDL VALUE WITH THE FACTOR K FOR TURBULENT FLOW IN CIRCULAR TUBES

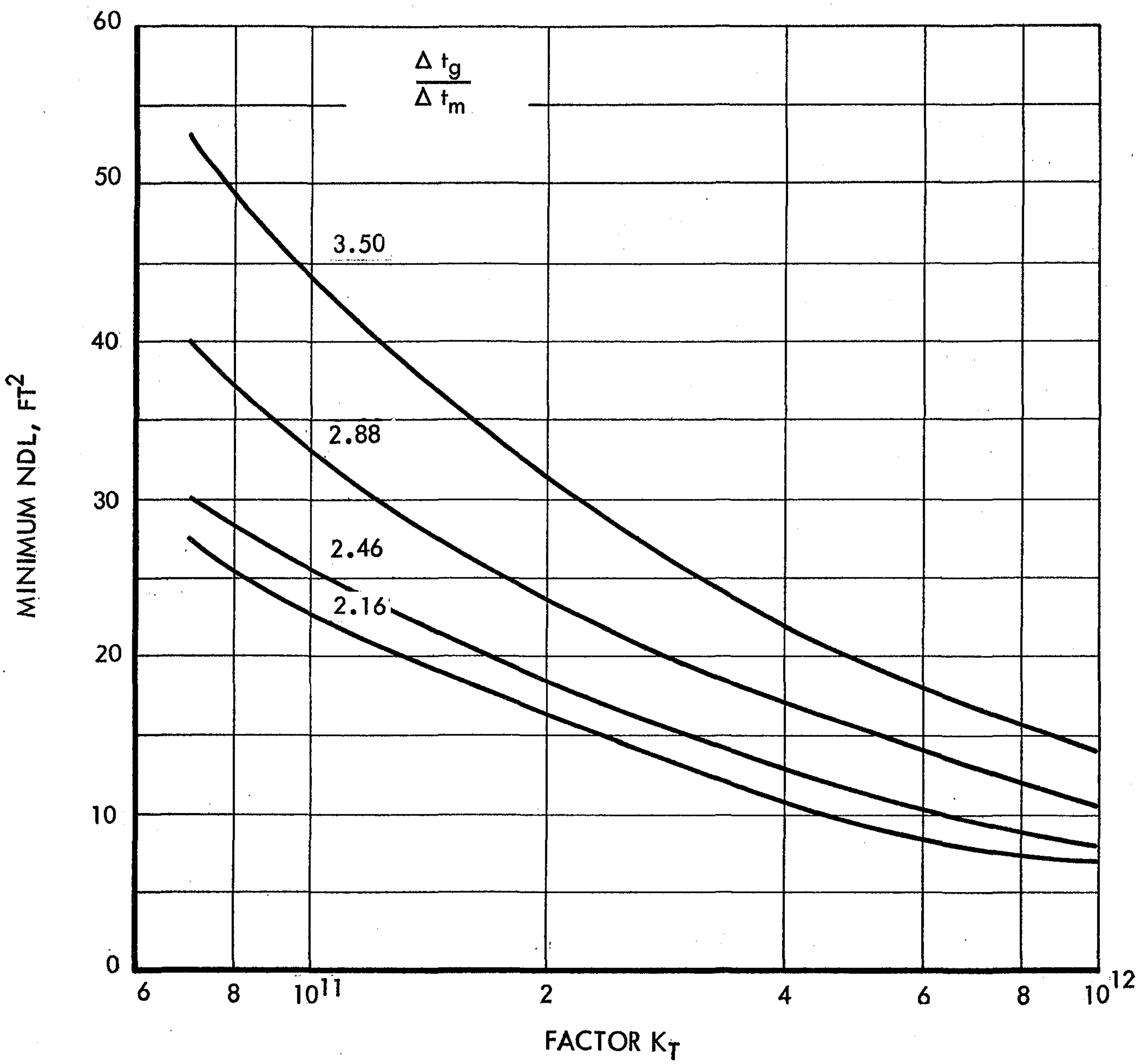

FIGURE 3

VARIATION OF THE FACTOR K FOR TURBULENT FLOW IN CIRCULAR TUBES WITH GAS SIDE TEMPERATURE DIFFERENCE AND PRESSURE DROP RATIO

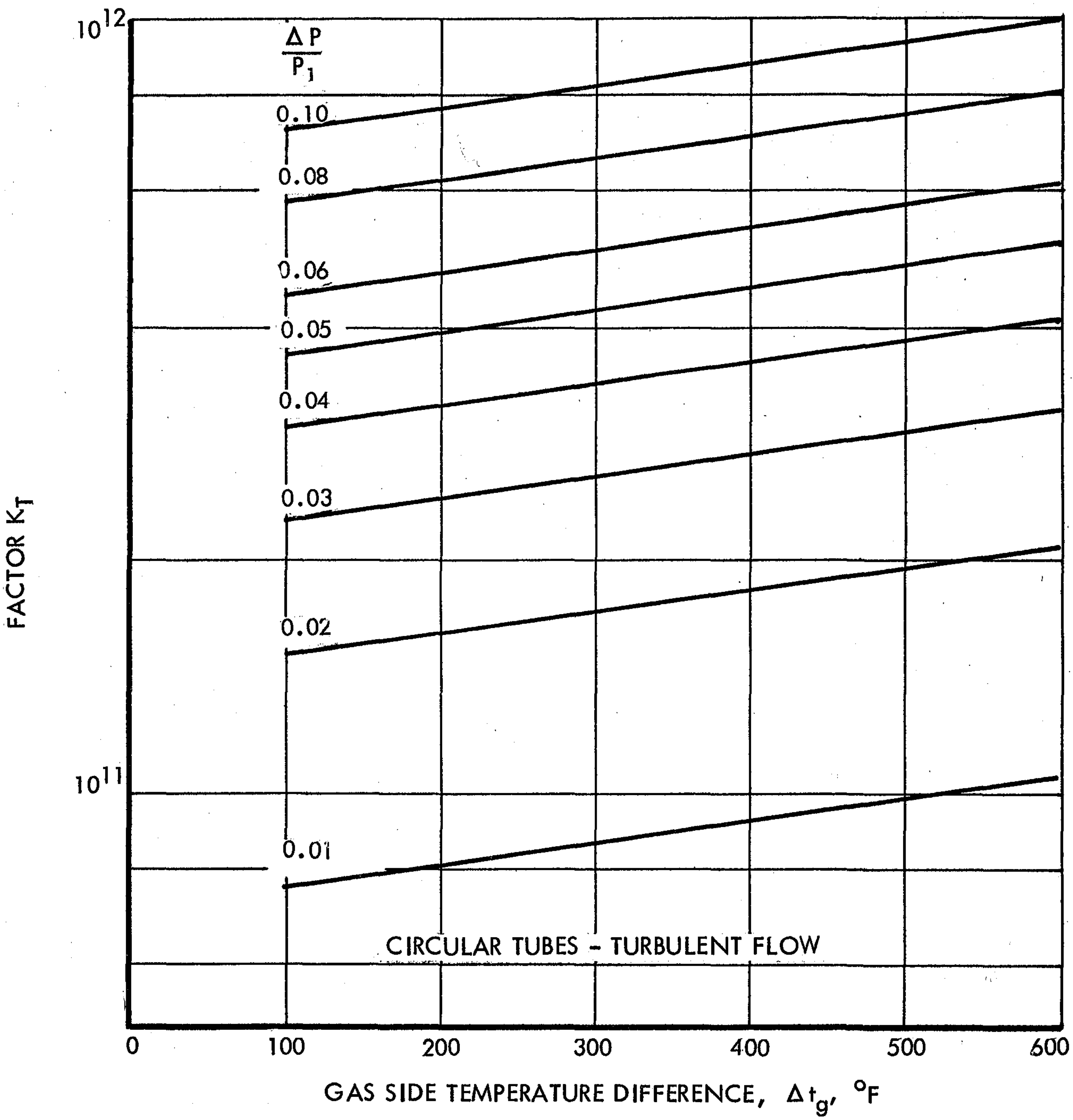

FIGURE 4

can be expected is approximately 0.4 of the manifold velocity head. When the irreversible friction loss in inlet and outlet headers of reasonable geometry is added to the entrance and exit losses, the total approaches one-half of the allowable pressure loss. Since the allowable percentage of pressure loss, specified in the preceding Table, is 4 percent of the inlet pressure, and one-half of this, or 2 percent, is needed for the headers, approximately 2 percent is available for the heater tubes. This level was employed in the above comparison.

The variation of the product NDL with Reynolds number at a given K_T is illustrated in Figure 5. It is interesting to note that the minimum occurred at the lowest Reynolds number. The same situation was encountered with K_L, where the minimum NDL occurred at 500, the lowest Reynolds number.

The level of the temperature difference ratio, $\Delta t_g/\Delta t_m$, required for any given design depends on the gas side temperature difference and the ratio $\Delta t_w/\Delta t_g$, in which Δt_w is the temperature difference between the wall temperature at the outlet and the wall temperature at the inlet. Figure 6 shows the expected range of variables for a 65°F temperature difference between the gas stream and the wall at the tube outlet. The temperature difference ratio, $\Delta t_w/\Delta t_g$, is a time-dependent variable. When the fluoride is all liquid, the wall temperature should be constant, and the above ratio would be zero. As the fluoride is allowed to freeze around the tube, the wall temperature at the inlet is decreased, and the wall temperature difference is finite. The ratio becomes greater than zero and increases with time in the shade. The heater must be designed to accommodate the maximum anticipated level of this ratio.

Typical results from the solution of the equations for a particular set of constants are presented in Figure 7. Figure 5 indicates that the product NDL increases with Reynolds numbers. Therefore, it is desirable to operate in a Reynolds number range close to 4,000, but the number of tubes for this type of operation creates serious packaging problems. The heater design then becomes a problem of selecting a combination of tube parameters that best fit given cavity shapes.

3.1.2 Storage Bath Design

The critical problem in a storage bath design is to provide the heat exchange required by the gas at the proper place and time. The heat exchange rate is governed by the total thermal resistance.

$$R_t = R_g + R_w + R_f$$

$$R_t = \frac{t_g - t_f}{Q/L}$$

$$R_g = \frac{1}{2\pi\, r_i\, h}$$

VARIATION OF THE PRODUCT NDL WITH REYNOLDS NUMBER
AT A CONSTANT K FACTOR LEVEL

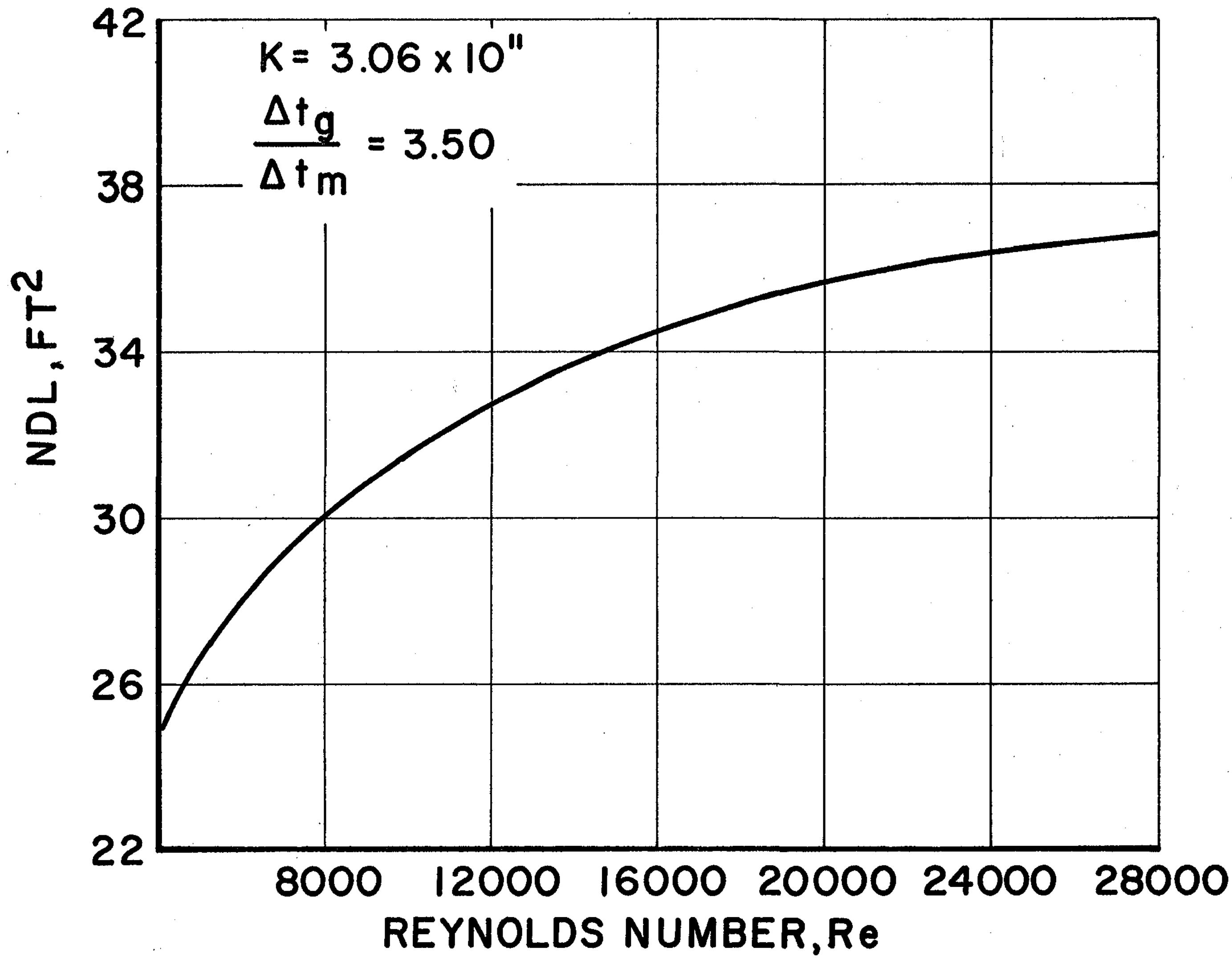

FIGURE 5

VARIATION OF GAS-TO-LOG MEAN TEMPERATURE DIFFERENCE RATIO WITH GAS SIDE TEMPERATURE DIFFERENCE FOR SEVERAL RATIOS OF WALL-TO-GAS TEMPERATURE DIFFERENCE AT A CONSTANT WALL-TO-GAS TEMPERATURE DIFFERENCE AT THE TUBE OUTLET OF 65°F

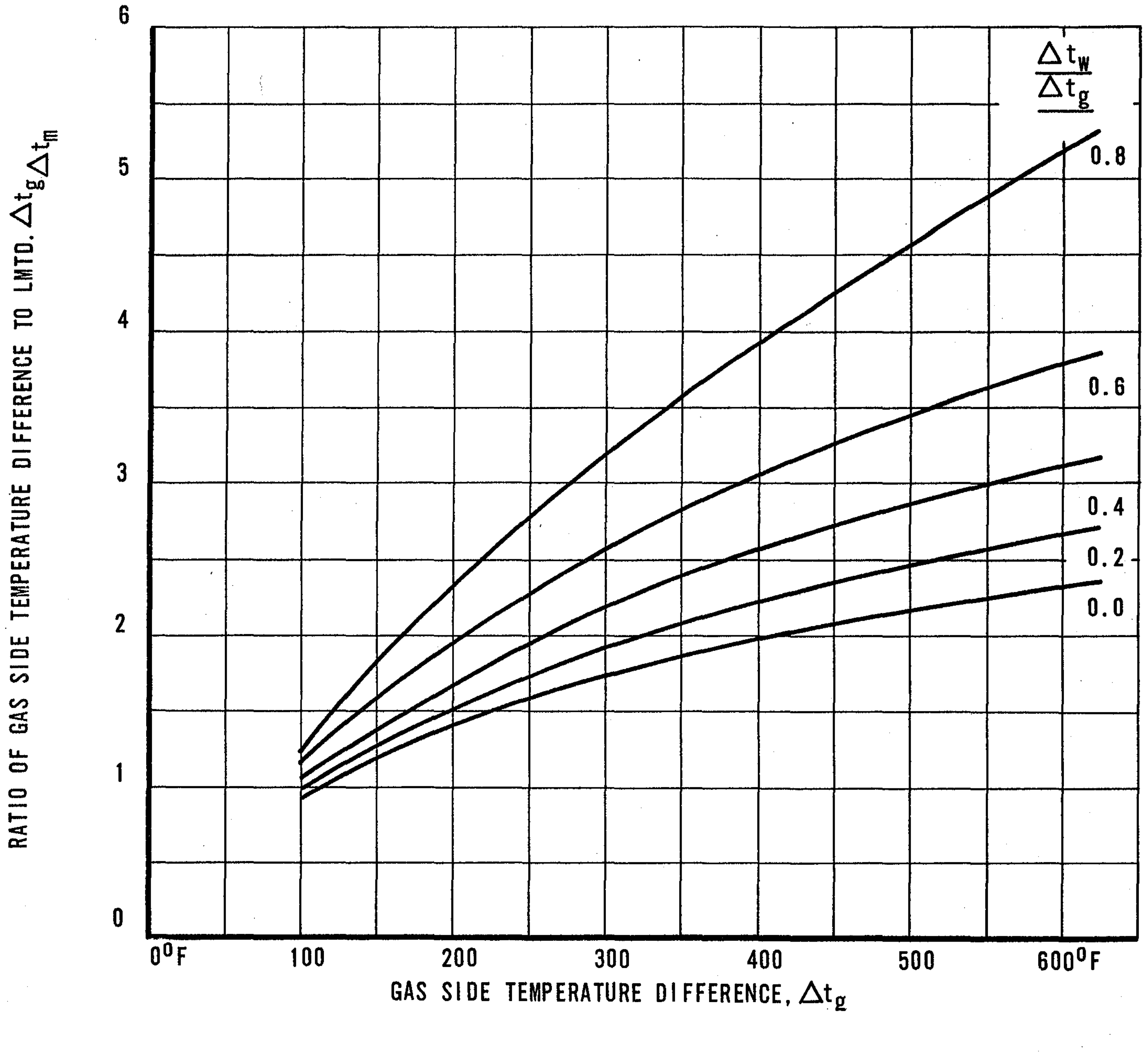

FIGURE 6

TYPICAL RESULTS FOR HEATER TUBE PARAMETERS
WITH TURBULENT FLOW IN CIRCULAR TUBES

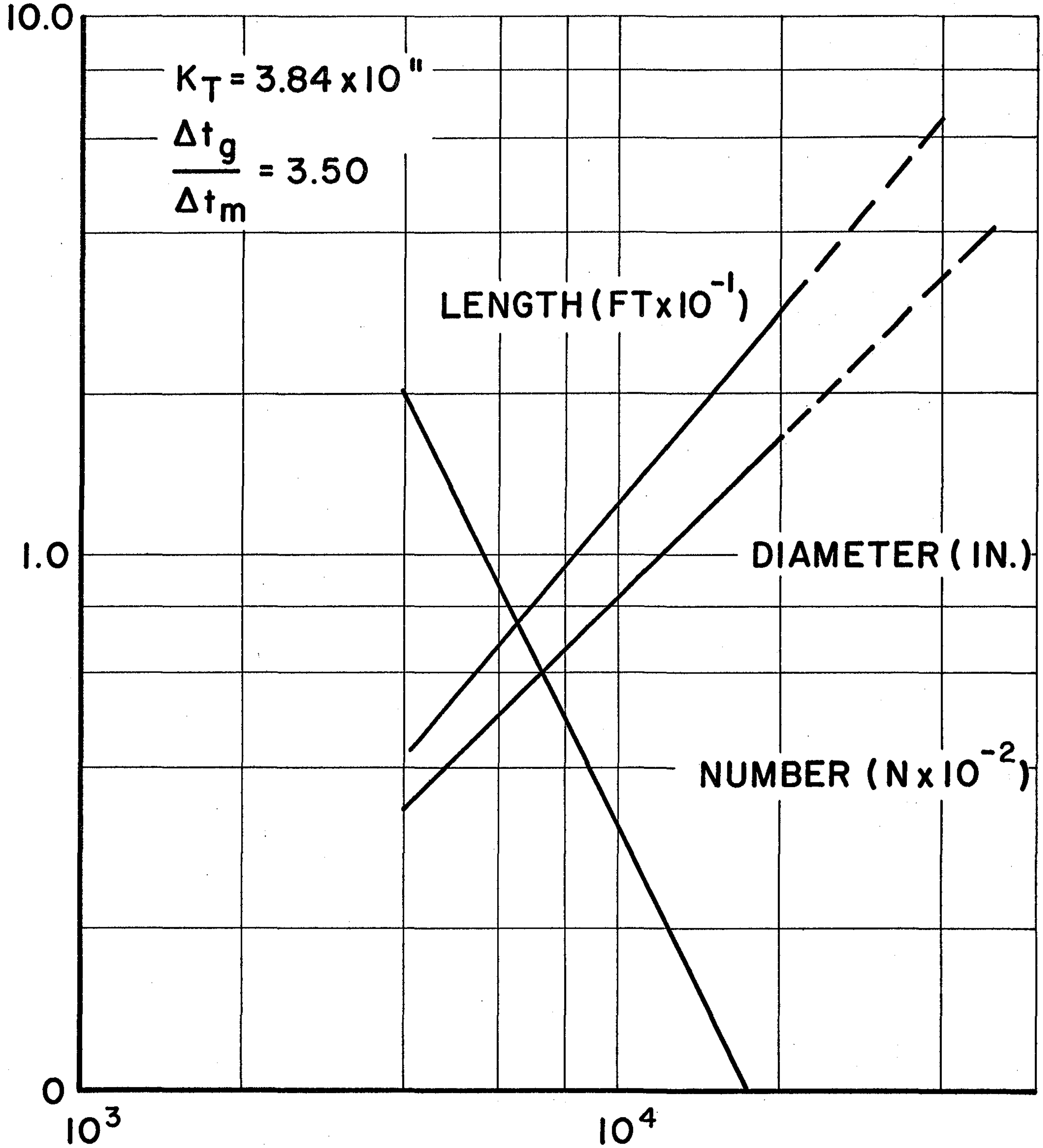

FIGURE 7

$$R_w = \frac{1}{2\pi k_w} \ln \frac{r_o}{r_i}$$

$$R_f = \frac{1}{2\pi k_f} \ln \frac{r_m}{r_o}$$

Where

R_t = total thermal resistance, ^{o}F-ft-hr/Btu

R_g = gas thermal resistance, ^{o}F-ft-hr/Btu

R_w = wall thermal resistance, ^{o}F-ft-hr/Btu

R_f = fluoride thermal resistance ^{o}F-ft-hr/Btu

t_f = fluoride melting temperature, ^{o}F

Q/L = heat transfer per unit length of tube, Btu/hr-ft

h = gas heat transfer coefficient, Btu/hr-sq. ft-^{o}F

k_w = wall thermal conductivity, Btu/hr-ft-^{o}F

k_f = fluoride thermal conductivity, Btu/hr-ft-^{o}F

r_i = tube inside radius, ft

r_o = tube outside radius, ft

r_m = radius to melt line, ft

The total thermal resistance depends on the fluoride resistance which, in turn, is determined by the thermal conductivity of the solid fluoride in the vicinity of the melting point. There are no known measurements of the thermal conductivity. An estimate is available from Reference 2. A theoretical value of the liquid conductivity calculated in Reference 3 is several times larger than the corresponding conductivity of lithium hydride. In view of this, the method proposed in Reference 3 is not recommended, because the higher molecular weight of lithium fluoride should result in lower conductivity. Thus, the total resistance and the fluoride resistance can only be approximated at this time.

The radius to the melt line increases with shade time and the fluoride resistance follows. The wall resistance is very small and can be ignored in preliminary design. The gas resistance is constant with time. Two typical situations encountered in the preliminary analysis are given in Figure 8. The two resistances are plotted versus the thickness of fluoride frozen for two designs. Since the gas resistance is greater than the fluoride

VARIATION OF THERMAL RESISTANCES WITH FROZEN FLUORIDE THICKNESS FOR TWO TYPICAL PRELIMINARY DESIGN CONFIGURATIONS

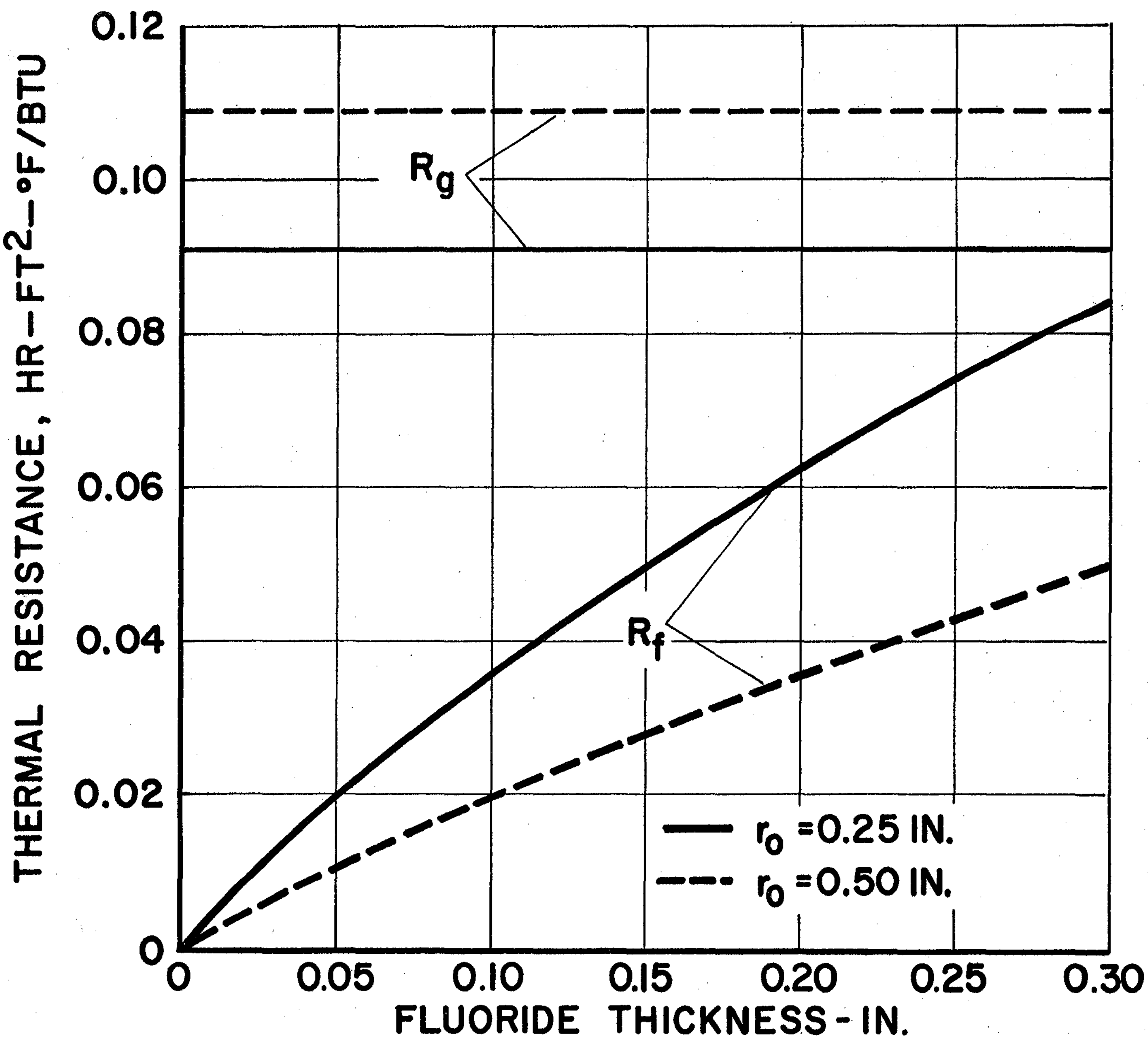

FIGURE 8

resistance at all times (Figure 8), the gas resistance is rate-controlling throughout.

Another aspect of the storage bath design is the total heat capacity needed. All designs made prior to the technical presentation were sized for 70 minutes of shade time corresponding to the synchronous orbit. Because of subsequent NASA redirection, later designs are being sized for 36 minutes and 70 minutes for the 300-mile orbit and the synchronous orbit, respectively. The heat capacity per pound of fluoride is the difference in enthalpy between that available at the maximum average bath temperature and the amount corresponding to the minimum average bath temperature. The influence of the minimum lithium fluoride temperature on the combined weight of the tubes and the fluoride is depicted in Figure 9 for several levels of the maximum gas temperature. The numbers indicated are for the 20,000-nautical-mile orbit.

3.1.3 Cavity Design

The critical item in the cavity design is the heat input rate to the fluoride. An estimate of the possible design input rate was made as follows:

$$g_{LiF} \approx g_{LiH} \frac{k_{Lif}}{k_{LiH}} = 10{,}000 \frac{1.5}{2.12}$$

$$\approx 7070 \text{ Btu/hr-sq. ft}$$

The cavity surface area for transferring heat to the fluoride must be equal to, or greater than, the quotient of heat input required in Btu/hr divided by 7070 Btu/hr-sq ft.

The cavity receiver designs which were evolved from the preliminary design analysis are shown in Figures 10, 11 and 12. Figure 10 is a design for a spherical fluoride container. Figure 11 features a cylindrical container and Figure 12 a conical one. The spherical cavity has the advantages of lightest possible weight and best cavity reception and retention. The cylinder is more readily fabricated, and the decrement in cavity performance is not significant at the low aperture-to-cavity surface area ratios anticipated. The conical container provides the smallest NDL product of the three designs, but the maximum diameter needed is greater than the design goal of 5 feet. The heater tube parameters are noted on each of the three figures.

3.2 Technical Presentation

A technical presentation setting forth the results of the preliminary design analysis was made on August 30, 1963. This presentation was performed exactly on schedule.

In accordance with the desired NASA redirection, the preliminary design analysis is continuing to identify suitable cavity receiver designs for single orbit operation. All designs shown herein, were made for multiple orbit operation and for any orbit between 300 and 20,000 nautical miles circular.

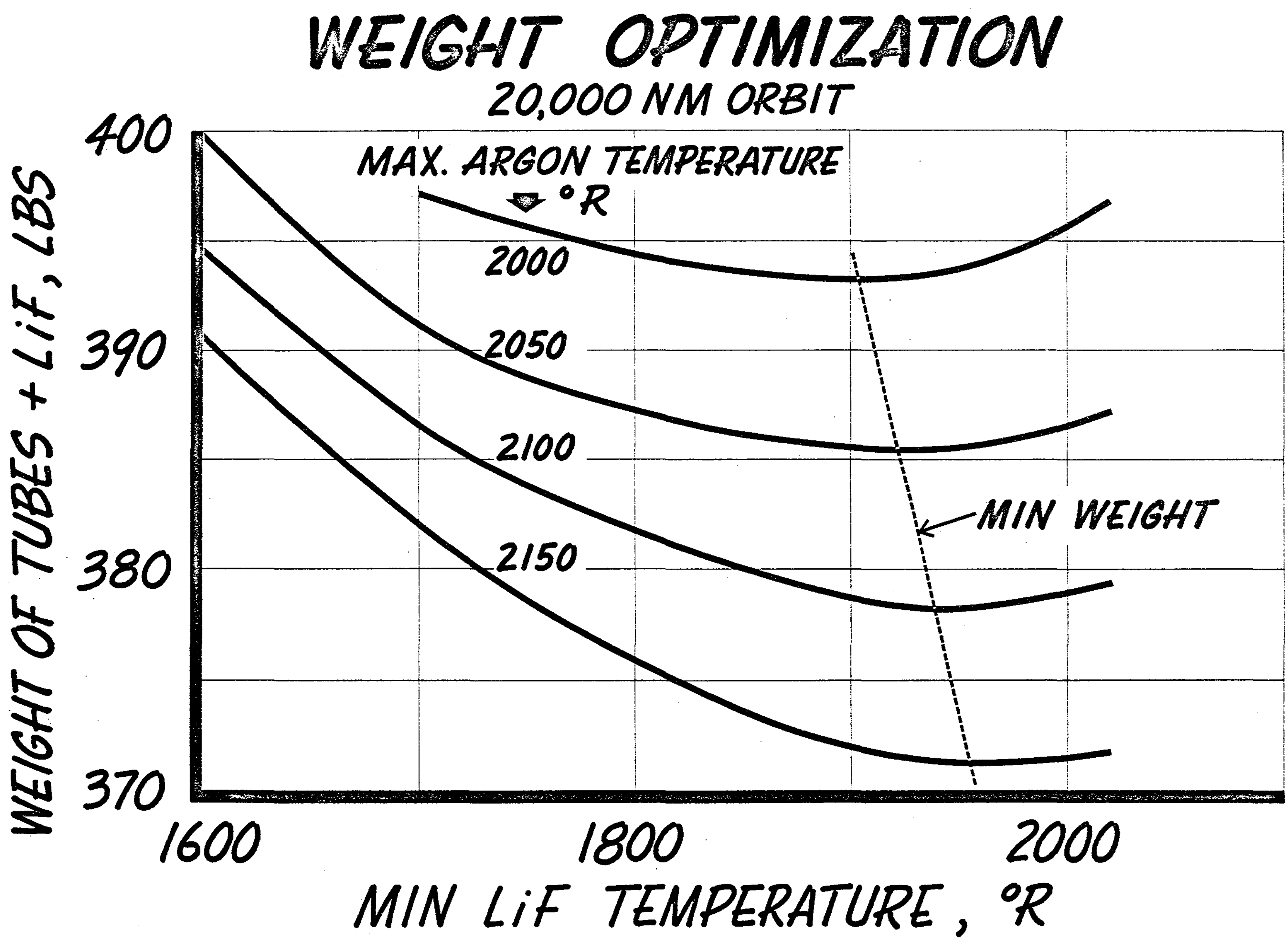

FIGURE 9

VARIATION OF THE TUBE AND FLUORIDE WEIGHT WITH THE MINIMUM FLUORIDE TEMPERATURE FOR SEVERAL LEVELS OF THE ARGON OUTLET TEMPERATURE

A

B

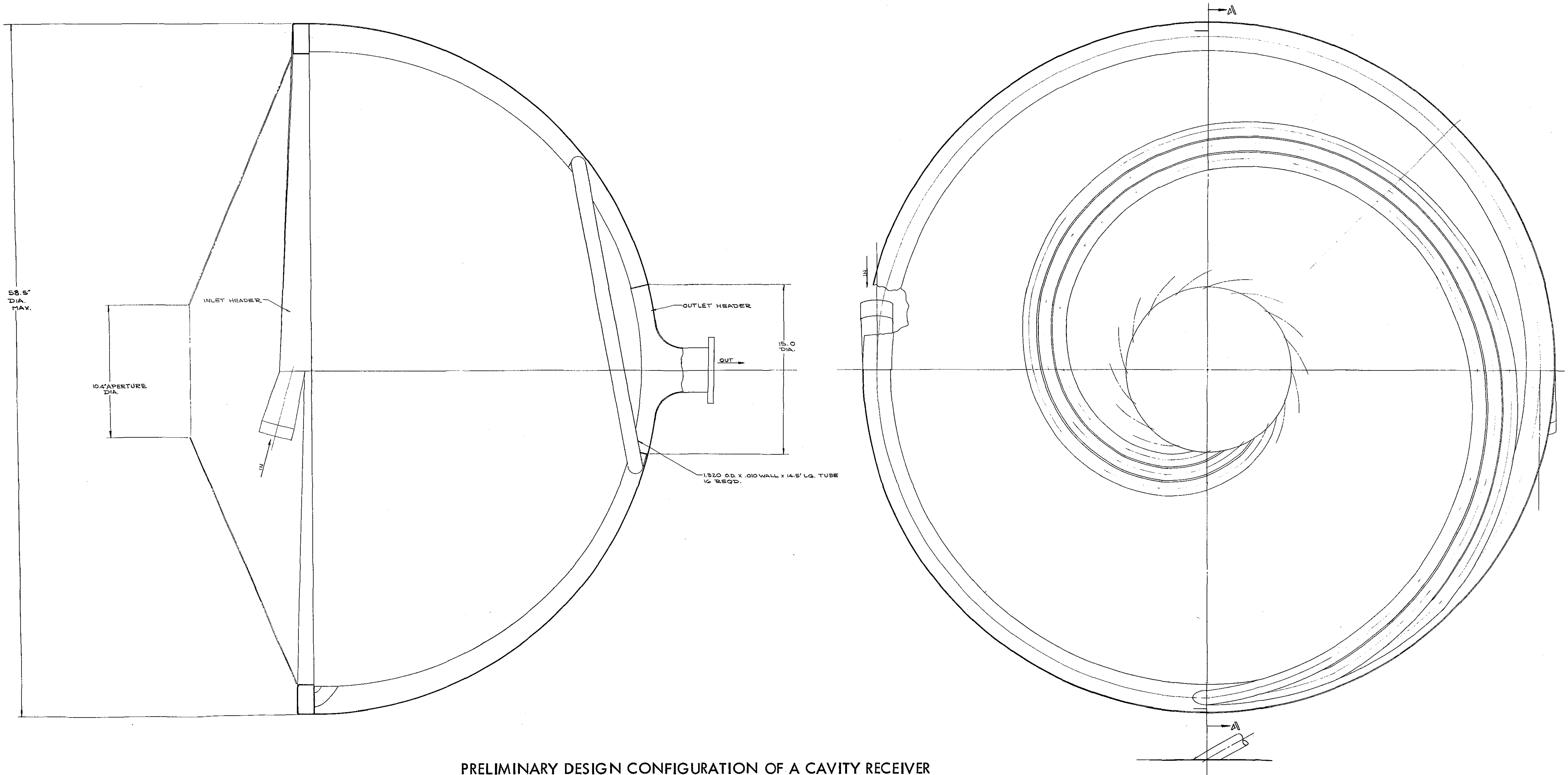

PRELIMINARY DESIGN CONFIGURATION OF A CAVITY RECEIVER
WITH A SPHERICAL FLUORIDE CONTAINER

FIGURE 10

PRELIMINARY DESIGN CONFIGURATION OF A CAVITY RECEIVER
WITH A CYLINDRICAL FLUORIDE CONTAINER

(B)

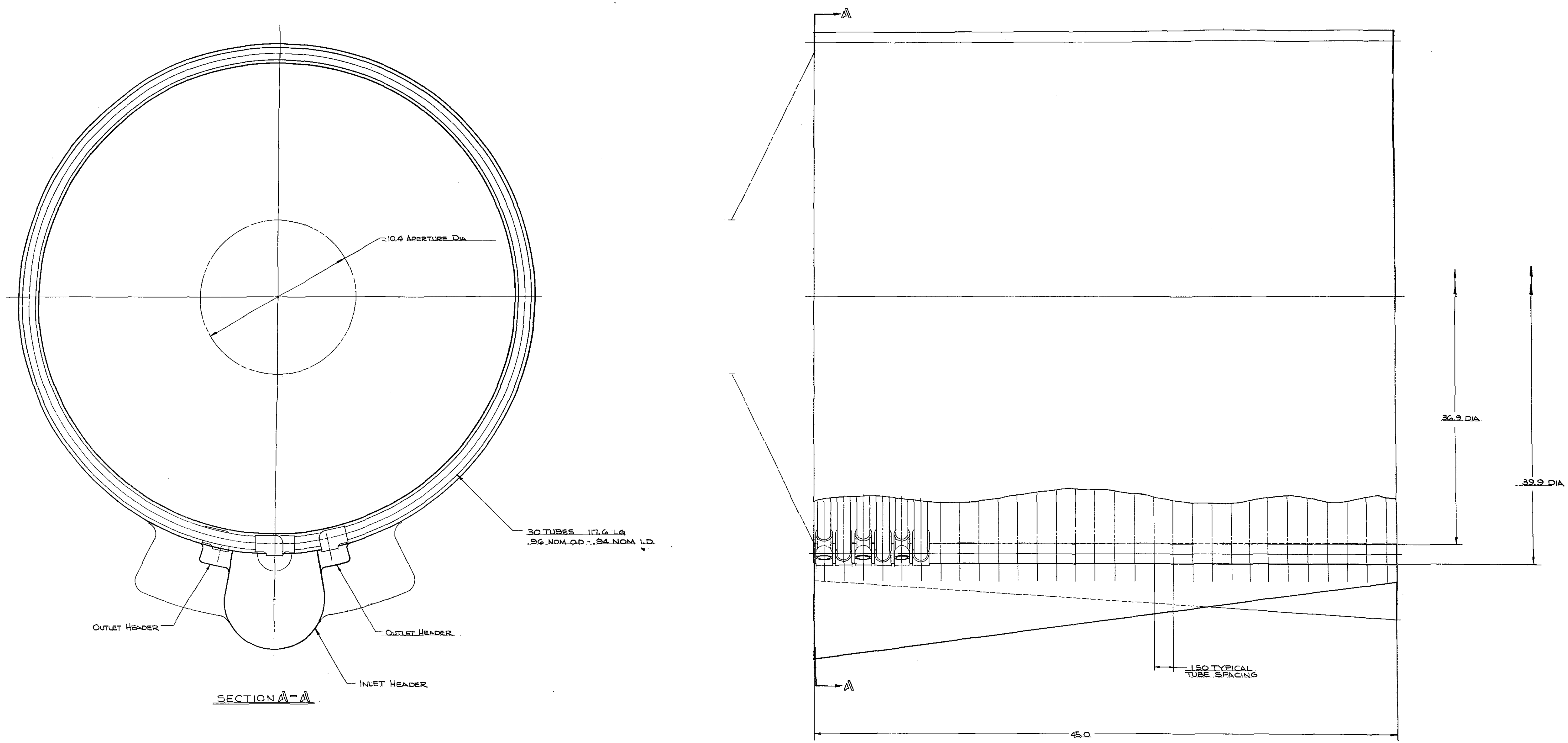

FIGURE 11

PRELIMINARY DESIGN CONFIGURATION OF A CAVITY RECEIVER
WITH A CONICAL FLUORIDE CONTAINER

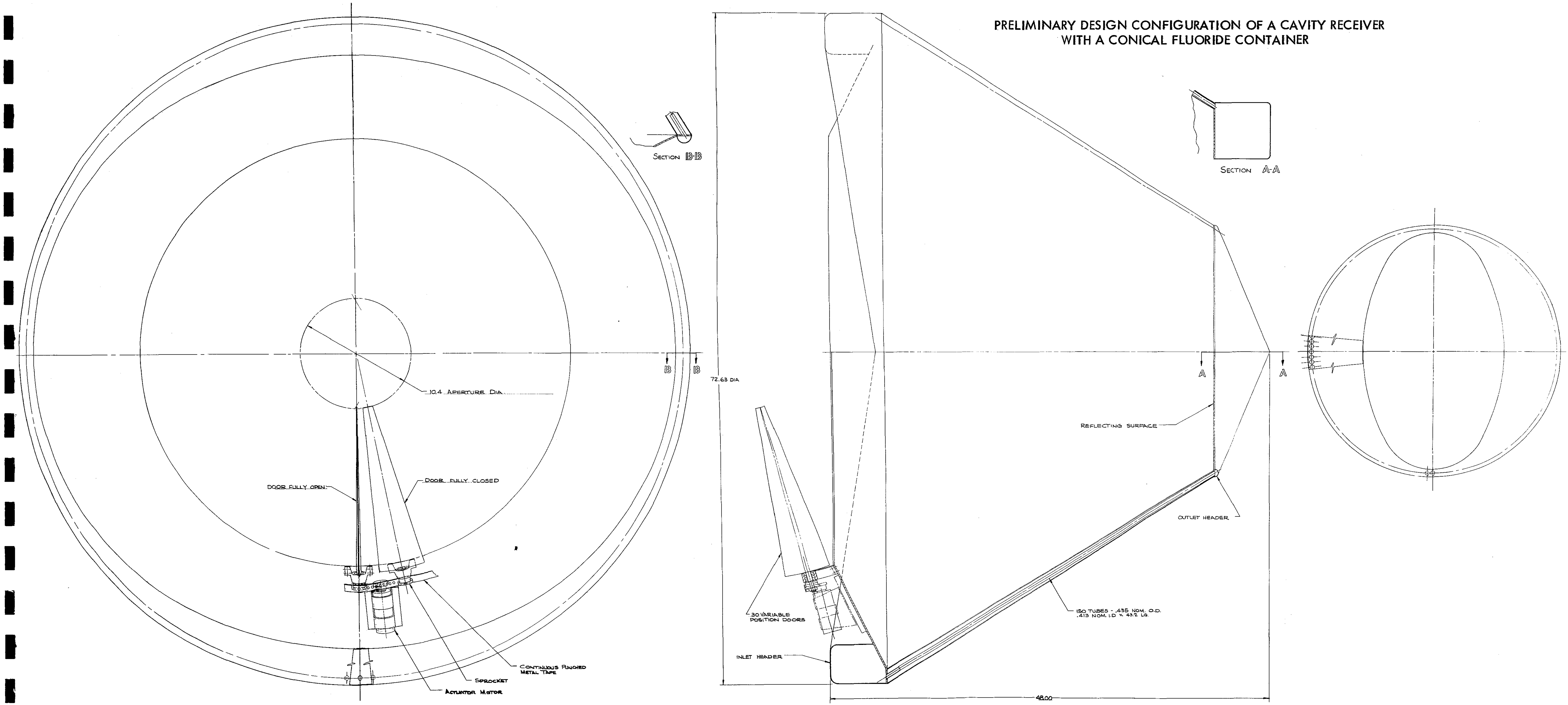

FIGURE 12

3.3 Small-Scale Experiments

Activity in this area was scheduled to start the second week of August. The actual start was delayed two weeks because of manpower needs. Progress has been satisfactory since that time. The test cell has been prepared; the modules have been designed; material for the first three units has been ordered and received; and a loading device is now being designed. The module designed for the unfinned unit is presented in Figure 13. Figure 14 shows a typical finned module.

The purpose of the tests to be conducted with the plain module is to determine the fluoride thermal conductivity of both the liquid and the solid in the vicinity of the melting point and to measure the heat input rates that can be attained. The tests with the finned modules are intended to demonstrate the increased heat input potential with fins.

3.4 Cavity Surface Temperature Control Study

A study of methods to control the cavity surface temperature and close the aperture during shade time operation was scheduled to start immediately after the technical presentation and was to employ the designs evolved in the analysis. Since the designs evolved were not the type of interest to NASA and new designs were required, this study has been deferred, pending definition of the new designs.

3.5 Lithium Fluoride Properties Investigation

The purpose of this investigation is to determine the handling, safety and purity requirements for lithium fluoride. In addition, data required for design of cavity receivers is to be collected and assessed.

This effort has had a low priority, but sufficient information has been obtained to define proper loading methods and the apparent safety and handling requirements. This investigation will continue during the next quarter.

3.6 Reliability

A reliability effort was initiated on schedule at a level necessary to satisfy the contractual requirements. The first item needed is a reliability plan for the entire program. At the present time, this plan is in the latter stages of preparation and should be available early next quarter.

No reliability analysis was conducted on the preliminary designs. The full-scale design, however, will be analyzed during the next quarter.

UNFINNED MODULAR CONFIGURATION FOR SMALL-SCALE EXPERIMENTS

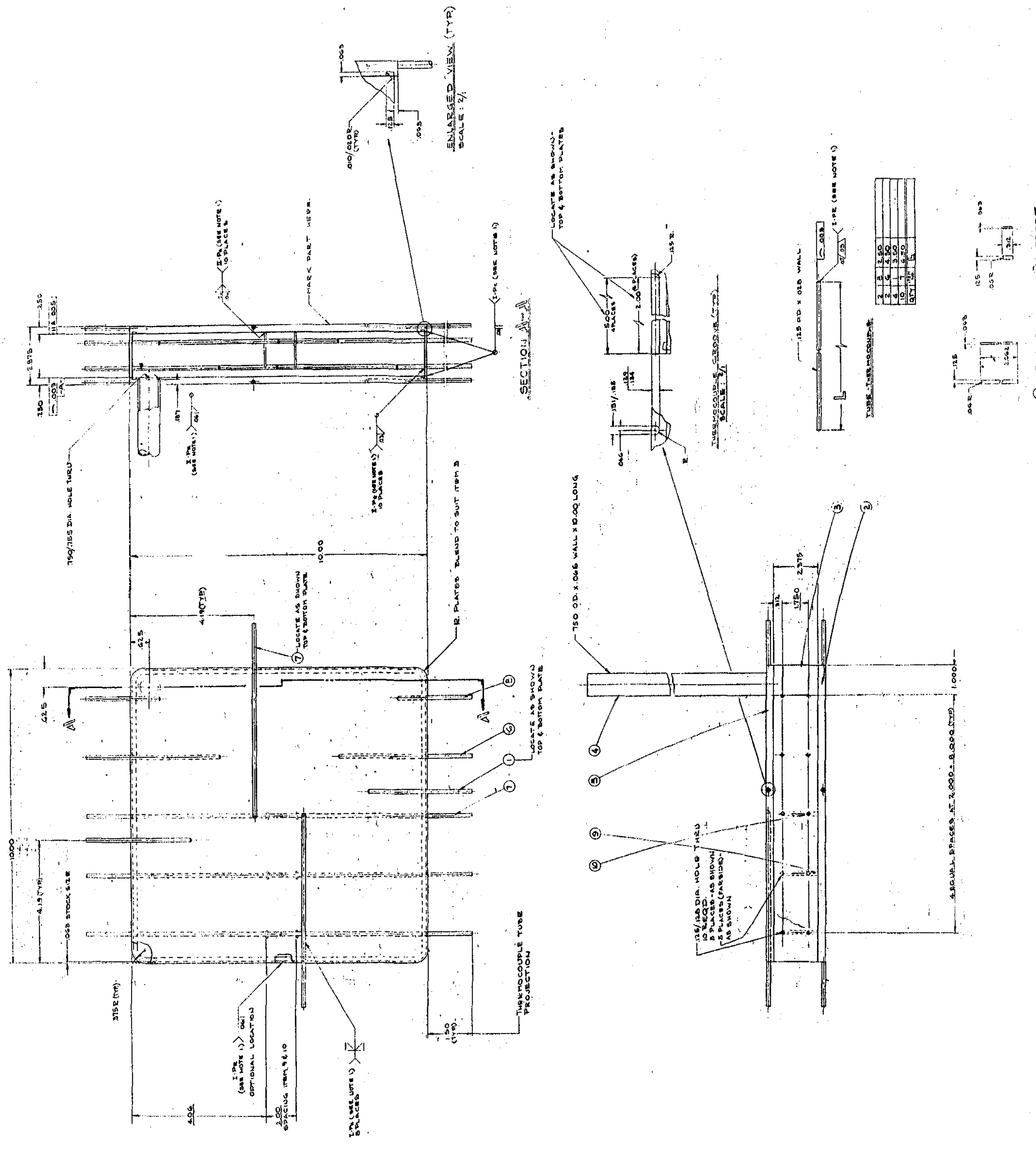

FIGURE 13

TYPICAL FIN MODULAR CONFIGURATION

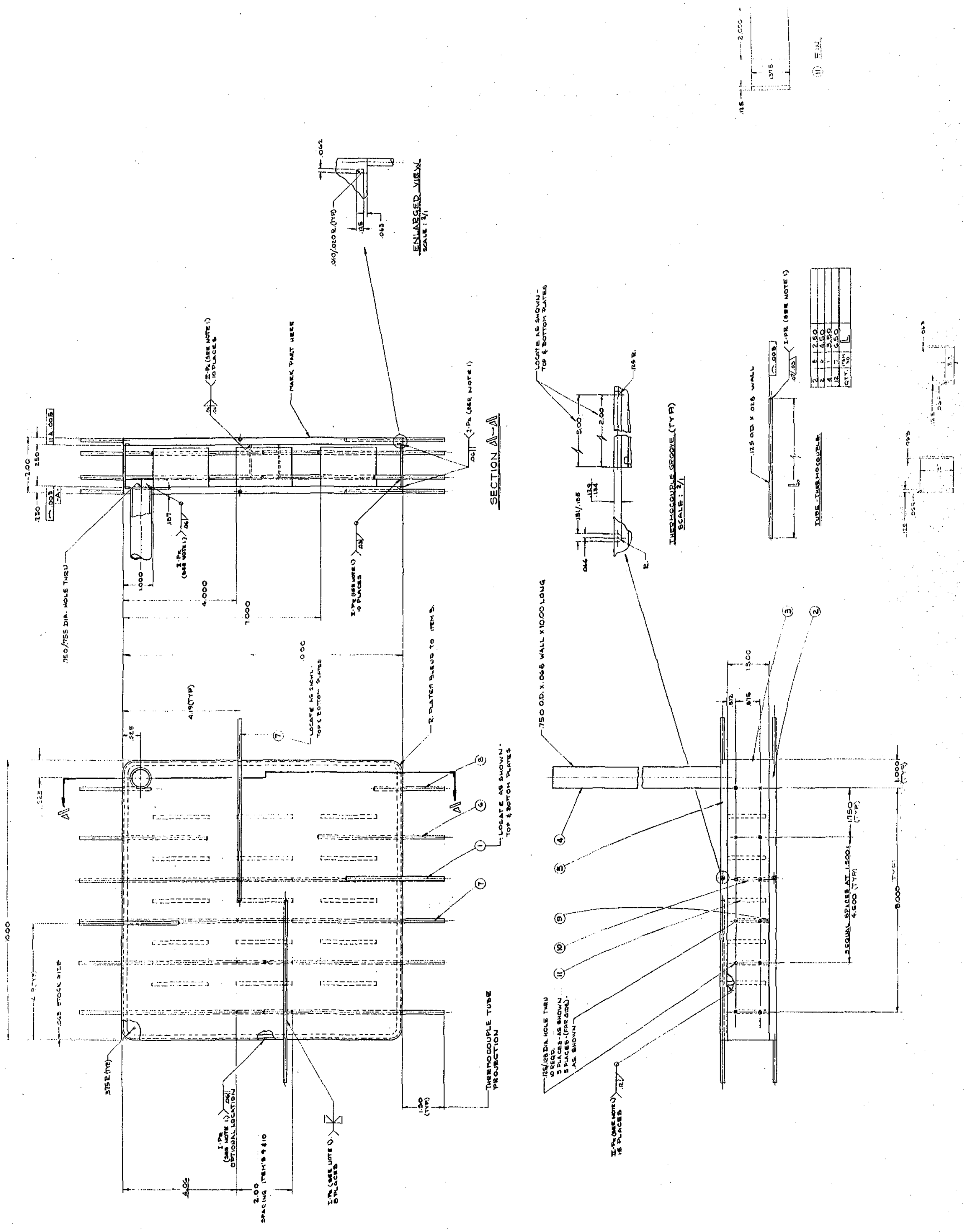

FIGURE 14

3.7 Materials Compatibility Investigation

Effort during the quarter was devoted to determination of the materials to be tested and the type of capsules to be fabricated, procurement of materials required, fabrication of the capsules and test containers, and preparation of the test furnace. Loading of the lithium fluoride into the test capsules will be accomplished after all capsules required for the first 2500-hour furnace test are fabricated.

A series of meetings were held between NASA and TRW representatives to select the test materials and the type of test capsules. Complete agreement was achieved between the representatives at each of the meetings, but formal direction as specified in the contract was not received by TRW during this quarter. It has been received early in the next quarter, prior to press time for this report. The delay of this document has resulted in a delay in capsule fabrication of two to four weeks. This delay will necessarily be incurred in the start of the first test.

All materials necessary for the first test have been ordered and received, with the sole exception of Haynes 56 bar stock needed for end caps. Two items, Rene 41 tubing and TD nickel bar stock, were supplied by NASA as government furnished material. The test materials specified by the formal letter of direction and the test capsule breakdown are as follows:

Alloy	Number and Type of Weld Configuration Capsules	Number of Brazed Capsules
Haynes 25	1 Capsule, End Caps Welded 2 Capsules, End Caps Welded With 2 Longitudinal Seam Welds	None
Haynes 56	2 Capsules, End Caps Welded With 2 Longitudinal Seam Welds	None
Waspalloy (Udimet 500)	Same as for Haynes 56	None
Hastelloy N (Hastelloy X)	Same as for Haynes 25	None
Rene 41	Same as for Haynes 25	2 Capsules, End Caps Brazed
TD Nickel	Same as for Haynes 25	2 Capsules, End Caps Brazed

The alloys Udimet 500 and Hastelloy X are optional, in case the other two cannot be obtained in time for furnace loading. Supplies of Waspalloy and Hastelloy N are on order, but have not been received at press time. Therefore, it is planned to employ Udimet 500 and Hastelloy X capsules in the first furnace test.

The lithium fluoride purchased for use in the capsules was ordered to the following specification:

Lithium Fluoride	99.5% Min.
SO_4	0.01 Max.
Iron as Fe_2O_3	0.02 Max.
Heavy Metals as Pb	0.001 Max.
Carbon Dioxide as Li_2CO_3	0.05 Max.
Weight Loss at 180°C	0.03 Max.

High Purity, 325 Mesh, in Moisture Proof Containers

The above specification is similar to the specification utilized by the Oak Ridge National Laboratory in their procurement of lithium fluoride.

Fabrication of the test capsules is in process with completion now forecast for 1 November. The capsules will be loaded with lithium fluoride at that time.

The capsule test containers were fabricated on schedule and are ready for insertion of the loaded capsules. The test furnace has been prepared and is ready for capsule container loading.

4.0 CURRENT PROBLEM AREAS

The only problem area which exists at the present time is the progress pace on the small-scale experiments. Concentrated effort will be made to speed up the fabrication, assembly and loading of the test modules so that the testing may begin at the earliest possible time. This area is the critical item in maintaining the program on schedule.

5.0 PLANNED DIRECTION OF EFFORT FOR THE NEXT QUARTER

During the next quarter, effort will be directed toward accomplishing these tasks:

1. The preliminary design analysis will be continued to identify single orbit designs for the 300-nautical-mile and the synchronous orbits.

2. The small-scale experiments will be performed and are scheduled for completion.

3. The cavity surface temperature control and aperture closure study will be initiated.

4. The fluoride properties investigation will be completed.

5. The reliability effort will be continued.

6. The first 2500-hour furnace test will be initiated with capsules made from the selected materials.

APPENDIX I: REFERENCES

1. "Second Quarterly Report on Experimental Investigation of Heat Rejection Problems in Nuclear Space Power Plants," (Contract NAS 3-2335), Report No. PWA-2132.

2. Wilson, H. W., Callery Chemical Co., Private Communication.

3. Brahm, K. W., Cooper, W. S., and Wilson, H. W., "Determination and Analysis of the Potentialities of Thermal Energy Storage Materials," June 30, 1961, ASD TR 61-187.

4. Drake, R. M., Jr. and Eckert, E.R.G., Heat and Mass Transfer, New York: McGraw Hill Book Co., Inc., 1959.

NOMENCLATURE FOR APPENDIX II

A = Heat transfer surface area, ft^2

A_c = Cross sectional flow area, ft^2

c_p = Specific heat at constant pressure, Btu/lb-^oR

D = Tube inside diameter, ft

D_h = Hydraulic diameter, ft

f = Friction factor, dimensionless

G = Mass velocity, lb/sec-ft

g_c = Gravitational conversion constant, lb_f-ft/lb_m-sec^2

h = Gas heat transfer coefficient, Btu/hr-sq. ft-^oF

K_L = Laminar factor $K = \frac{2g_c}{64} \cdot \frac{\Delta P \bar{\rho}}{\bar{\mu}^2}$

K_T = Turbulent factor $K = \frac{2g_c}{0.316} = \frac{\Delta P \bar{\rho}}{\bar{\mu}^2}$

k_f = Fluoride thermal conductivity, Btu/hr-ft-^oF

k_w = Wall thermal conductivity, Btu/hr-ft-^oF

L = Tube length, ft

N = Number of tubes

Nu = Nusselt number, dimensionless

P = Passage perimeter, ft

ΔP = Allowable pressure drop, lb/ft^2

Pr = Prandtl number, dimensionless

Q/L = Heat transfer per unit length of tube, Btu/hr-ft

Q_H = Heater duty, Btu/hr

Re = Reynolds number, dimensionless

R_f = Fluoride thermal resistance, °F-ft-hr/Btu

R_g = Gas thermal resistance, °F-ft-hr/Btu

R_t = Total thermal resistance, °F-ft-hr/Btu

R_w = Wall thermal resistance, °F-ft-hr/Btu

r_i = Tube inside radius, ft

r_m = Radius to melt line, ft

r_o = Tube outside radius, ft

S_t = Stanton number, dimensionless

t_f = Fluoride melting temperature, °F

$\Delta t_g - t_{g,2} - t_{g,1}$ = Gas side temperature difference

Δt_m = Log mean temperature difference between tube wall and gas stream

w. = Weight flow, lb/hr

$\bar{\mu}$ = Average absolute viscosity, lb/sec-ft

$\bar{\rho}$ = Average density, lb/ft^3

APPENDIX II: DERIVATION OF HEATER EQUATIONS

The equations employed in the heater preliminary design analysis were derived in the following manner:

The heater duty is $Q_H = wc_p \Delta t_g = hA\Delta t_m$

$$\therefore \quad \frac{hA}{wc_p} = \frac{\Delta t_g}{\Delta t_m}$$

$$\frac{hA}{wc_p} = \frac{h\,(A/A_c)}{c_p\,(w/A_c)} = \frac{h}{3600\,G\,c_p}\,\frac{A}{A_c} = St\,\frac{A}{A_c}$$

For circular tubes,

$$\frac{A}{A_c} = 4\,\frac{L}{D}$$

$$\therefore \quad \frac{\Delta t_g}{\Delta t_m} = 4St\,\frac{L}{D}$$

In laminar flow,

$$St = \frac{Nu}{Pr\,Re} = \frac{4.12}{0.7\,Re} = \frac{5.886}{Re}$$

$$Pr = 0.7 \text{ for gases}$$

$$\frac{\Delta t_g}{\Delta t_m} = \frac{5.886}{Re}\,4\,\frac{L}{D} = \frac{23.544}{Re}\,\frac{L}{D}$$

In turbulent flow,

$$St = \frac{0.0384\,Re^{-1/4}}{1 + 1.78\,Re^{-1/8}\,(Pr-1)} \quad \text{(Reference 4)}$$

$$= \frac{0.0384\,Re^{-1/4}}{1 - 0.534\,Re^{-1/8}}$$

$$4St\,\frac{L}{D} = \frac{0.1536\,Re^{-1/4}}{1-0.534\,Re^{-1/8}}\;\frac{L}{D} = \frac{\Delta t_g}{\Delta t_m}$$

The friction pressure drop is:

$$\Delta P = f\,\frac{L}{D}\;\frac{G^2}{\bar{\rho}\;2g_c}$$

For circular tubes:

In laminar flow,

$$f = \frac{64}{Re}$$

$$G = \frac{Re\,(\bar{\mu})}{D}$$

$$\Delta P = \frac{64}{Re}\;\frac{L}{D}\;\frac{Re^2\;\bar{\mu}^2}{D^2\,\bar{\rho}\,2g_c}$$

$$Re\,\frac{L}{D}\;\frac{1}{D^2} = \frac{\Delta P\;\bar{\rho}\;2g_c}{64\,\bar{\mu}^2} = K_L$$

In turbulent flow,

$$f = \frac{0.316}{Re^{1/4}}$$

$$\Delta P = \frac{0.316}{Re^{1/4}}\;\frac{L}{D}\;\frac{Re^2\;\bar{\mu}^2}{D^2\,\bar{\rho}\;2g_c}$$

$$Re^{1.75}\,\frac{L}{D}\;\frac{1}{D^2} = \frac{\Delta P\;\bar{\rho}\;2g_c}{0.316\;\bar{\mu}^2} = K_T$$

The definition of Reynolds number in a tube is:

$$Re = \frac{GD}{\bar{\mu}}$$

$$G = \frac{w}{3600 A_c} = \frac{w}{3600N \frac{\pi}{4} D^2} = \frac{4w}{3600 \pi D^2 N}$$

$$Re = \frac{4w}{3600\pi D^2 N} \frac{D}{\bar{\mu}} = \frac{4w}{3600\pi D N \bar{\mu}}$$

$$\therefore \quad Re\, N D = \frac{4w}{3600 \pi \bar{\mu}}$$

For rectangular tubes,

$$D = D_h = \frac{4 A_c}{P}$$

$$AR = \text{Aspect Ratio} = \frac{\text{long side}}{\text{short side}} = \frac{b}{a}$$

$$A_c = ab = a^2 AR$$

$$P = 2(a + b) = 2a(1 + AR)$$

$$\therefore \quad D_h = \frac{4 A_c}{P} = \frac{4 a^2 AR}{2a(1 + AR)} = \frac{2a AR}{1 + AR}$$

The aspect ratio was varied from 2 to 12 in increments of 2 in an attempt to find a configuration amenable to a spherical container. No significant improvement was obtained, however, and this approach was discarded in view of the fabrication problems associated with rectangular tubes.

DISTRIBUTION LIST

Copy No.	
1	National Aeronautics & Space Administration 1512 H Street, Northwest Washington 25, D.C. Attention: Walter Scott (RP)
2	National Aeronautics & Space Administration 1512 H Street, Northwest Washington 25, D.C. Attention: Herbert Rochen (RNEP)
3	National Aeronautics & Space Administration 1512 H Street, Northwest Washington 25, D.C. Attention: George Deutsch
4	Lewis Research Center National Aeronautics & Space Administration 21000 Brookpark Road Cleveland 35, Ohio Attention: Dr. Bernard Lubarsky
5	Lewis Research Center National Aeronautics & Space Administration 21000 Brookpark Road Cleveland 35, Ohio Attention: R. L. Cummings
6	Lewis Research Center National Aeronautics & Space Administration 21000 Brookpark Road Cleveland 35, Ohio Attention: Dr. Louis Rosenblum
7	Lewis Research Center National Aeronautics & Space Administration 21000 Brookpark Road Cleveland 35, Ohio Attention: D. C. Guentert

Copy No.	
8	Lewis Research Center National Aeronautics & Space Administration 21000 Brookpark Road Cleveland 35, Ohio Attention: J. A. Heller
9, 10	Lewis Research Center National Aeronautics & Space Administration 21000 Brookpark Road Cleveland 35, Ohio Attention: J. A. Milko
11	Lewis Research Center National Aeronautics & Space Administration 21000 Brookpark Road Cleveland 35, Ohio Attention: T. A. Moss
12	Lewis Research Center National Aeronautics & Space Administration 21000 Brookpark Road Attention: R. P. Krebs
13	Lewis Research Center National Aeronautics & Space Administration 21000 Brookpark Road Cleveland 35, Ohio Attention: J. J. Fackler
14	Lewis Research Center National Aeronautics & Space Administration 21000 Brookpark Road Cleveland 35, Ohio Attention: N. T. Musial
15	Ames Research Center National Aeronautics & Space Administration Moffett Field, California Attention: Librarian
16	Goddard Space Flight Center National Aeronautics & Space Administration Washington 25, D.C. Attention: Librarian

Copy No.	
17	Langley Research Center National Aeronautics & Space Administration Hampton, Virginia Attention: Librarian
18	Marshall Space Flight Center National Aeronautics & Space Administration Huntsville, Alabama Attention: Librarian
19	Lewis Research Center National Aeronautics & Space Administration 21000 Brookpark Road Cleveland 35, Ohio Attention: Librarian
20	National Bureau of Standards Washington 25, D.C. Attention: Librarian
21	U.S. Naval Research Laboratory Washington 25, D.C. Attention: Librarian
22	Jet Propulsion Laboratory California Institute of Technology Pasadena, California Attention: Librarian
23	Air Force Systems Command Aeronautical Systems Division Wright Patterson Air Force Base, Ohio Attention: G. Thompson
24	Air Force Systems Command Aeronautical Systems Division Wright Patterson Air Force Base, Ohio Attention: Librarian
25	U.S. Atomic Energy Commission Technical Reports Library Washington 25, D.C. Attention: Librarian

Copy No.	
26	U.S. Atomic Energy Commission Technical Information Extension P.O. Box 62 Oak Ridge, Tennessee Attention: Librarian
27	Union Carbide Nuclear Co. X-10 Laboratory P.O. Box X Oak Ridge, Tennessee Attention: J. H. DeVon
28	Union Carbide Nuclear Co. X-10 Laboratory P.O. Box X Oak Ridge, Tennessee Attention: E. E. Hoffman
29	Union Carbide Nuclear Co. X-10 Laboratory P.O. Box X Oak Ridge Tennessee Attention: Librarian
30	Argonne National Laboratories Lemont, Illinois Attention: Librarian
31	Battelle Memorial Institute 505 King Ave. Columbus, Ohio Attention: Librarian
32	Armour Research Foundation Technical Center Chicago, Illinois Attention: Librarian
33	AiResearch Manufacturing Division The Garrett Corporation Phoenix, Arizona Attention: Librarian

Copy No.	
34	Allison Division General Motors Corporation Indianapolis 6, Indiana Attention: Librarian
35	General Electric Company Missile & Space Vehicle Department 3198 Chestnut Street Philadelphia 4, Pennsylvania Attention: Librarian
36	Electro-Optical Systems, Inc. 125 N. Vinedo Avenue Pasadena, California Attention: Librarian
37	Space Technology Laboratories P.O. Box 95001 Los Angeles 45, California Attention: Librarian
38	Sunstrand Denver 2480 W. 70th Avenue Denver 21, Colorado Attention: Librarian
39	Aerojet General Corporation Azusa, California Attention: Librarian
40	Pratt & Whitney Aircraft 400 Main Street E. Hartford, Connecticut Attention: Librarian
41	Pratt & Whitney Aircraft CANEL Middletown, Connecticut Attention: Librarian
42	General Electric Company FPLD Cincinnati, Ohio Attention: Librarian

Copy No.	
43	MSA Research Corporation Callery, Pennsylvania Attention: Librarian
44	Lithium Corporation of America Inc. Bessemer City, North Carolina Attention: Librarian
45	Foote Mineral Company Philadelphia, Pennsylvania Attention: Librarian
46	Bendix Corporation Southfield, Michigan Attention: G. T. Burton
47	Department of Engineering University of California Los Angeles, California Attention: Librarian
48	Manned Space Center National Aeronautics & Space Administration Houston, Texas Attention: Librarian
49, 50 plus reproducible	National Aeronautics & Space Administration Scientific and Technical Information Center Box 5700 Bethesda 14, Maryland Attention: NASA Representative